

Assessment of Two Wall Film Condensation Models of RELAP5/MOD3.2 in the Presence of Noncondensable Gas in a Vertical Tube

Hyun Sik PARK and Hee Cheon NO

Korea Advanced Institute of Science and Technology
373-1 Ku-song Dong, Yu-song Gu, Taejon 305-701, Korea
hspark@nesun1.kaist.ac.kr

Young Seok BANG

Korea Institute of Nuclear Safety
19 Ku-song Dong, Yu-song Gu, Taejon 305-338, Korea

(Received May 21, 1999)

Abstract

The objective of the present work is to assess the analysis capability of two wall film condensation models, the default and the alternative models, of RELAP5/MOD3.2 on condensation experiments in the presence of noncondensable gas in a vertical tube of PCCS of CP-1300. In the calculation of a base case the default model of RELAP5/MOD3.2 under-predicts the heat transfer coefficients, and its alternative model over-predicts them throughout the condensing tube. Also, both models over-predict the void fractions. The nodalization study shows that the variation of the node number does not change both modeling results of RELAP5/MOD3.2. Sensitivity study for varying input parameters shows that the inlet steam-air mixture flow rate, the inlet air mass fraction, and the inlet saturated steam temperature give significant changes of their heat transfer coefficients. Run statistics show that the grind time of the default model is always higher than that of the alternative model by about 23%.

Key Words : RELAP5/MOD3.2, film condensation, noncondensable gas

1. Introduction

CARR (Center for Advanced Reactor Research) develops CP-1300[1] (CARR Passive Reactor), a next generation reactor, which is a large passive pressurized water reactor concept. It has a concrete containment and the final safety

functions are achieved through various passive systems such as accumulator, Core Makeup Tank (CMT), Secondary Condenser (SC) and Passive Containment Cooling System (PCCS). CP-1300 adopts the external condenser concept[2] as its PCCS. It uses the condensation of steam in condensing tubes, which are located in a water

pool outside a containment. In the design of PCCS the capability to deal with steam-noncondensable gas mixtures in vertical tubes is an important technical problem. As steam-noncondensable gas mixture enters into a vertical condensing tube of PCCS, steam begins to condense at the inlet of the tube. The steam condenses on the inner wall of the tube and the condensate film flows as an annular film along the condensing tube. A gas-vapor boundary layer forms next to the condensate interface, through which the water vapor must pass by diffusion and convection, and it thickens between the condensate film layer and the steam-noncondensable gas mixture layer. Choi et al.[3] assessed both wall film condensation models in RELAP5/MOD3.2[4] based on the condensation database, which is constructed from the previous experimental data. The assessment shows that the two models predict quite different heat transfer coefficients compared with the database.

The main objective of the present work is to assess and compare the capability of both models in RELAP5/MOD3.2. Both Siddique et al.[5] and Kuhn[6] performed air-steam experiments and developed their own correlations, but their ranges of experimental parameters were very different. At KAIST the condensation experiments[7] are performed with the steam-noncondensable gas mixture in a vertical tube representing condensing tubes in PCCS. The experimental parameters have wider ranges than those of previous works. The assessment is performed on one of their experiments, E12b, as a base case. Both of the nodalization study and the sensitivity study are performed.

2. Two Wall Film Condensation Models of Relap5/MOD3.2

RELAP5/MOD3.2 has two wall film

condensation models, the default and the alternative models. The default model uses the Nusselt-Shah-Colburn-Hougen correlations, and the alternative model uses the Nusselt-UCB correlations for the wall film condensation on an inclined surface.

The default model uses the maximum of the Nusselt[8] and Shah[9] correlations with the Colburn-Hougen[10]'s diffusion calculation when noncondensable gases are present. In Nusselt expression[8] for the vertical surfaces the film thickness is

$$h_f = \frac{k_f}{\delta}, \quad (1)$$

where h_f is the heat transfer coefficient, k_f the thermal conductivity, and δ the thickness of the condensate film. The Shah model[9] is used for the modeling of film condensation with turbulent flow in RELAP5/MOD3.2. However, as the condensate film is in laminar flow regime in the condensing tubes of PCCS, the Nusselt correlation is always used instead of the Shah model.

The formulation of the Colburn-Hougen model is based on the principle that the amount of heat transferred by condensing vapor to the liquid-vapor interface by diffusing through the noncondensable gas film is equal to the heat transferred through the condensate. The heat flux due to vapor mass flux, q''_v , is expressed as follows:

$$q''_v = h_m i_{fgb} \rho_{vb} \ln \left[\frac{1 - P_{vi}/P}{1 - P_{vb}/P} \right], \quad (2)$$

where h_m is the mass transfer coefficient, i_{fgb} the enthalpy of evaporation in the bulk, ρ_{vb} the saturated vapor density in the bulk, P the total pressure, P_{vi} the partial pressure of steam at liquid-gas-vapor interface, and P_{vb} the partial pressure of steam in the bulk. The mass transfer coefficient, h_m , depends on the flow condition. When the

vapor flow is turbulent and laminar, the Gilliland and Rohsenow-Choi correlations[11] are used, respectively. The heat flux from the liquid to the wall, q_1'' , is calculated by

$$q_1'' = h_f \cdot (T_{vi} - T_w) , \quad (3)$$

where T_{vi} is the saturated vapor temperature of the liquid-gas-vapor interface and T_w the surface temperature of the wall. From the energy balance the partial vapor pressure at the interface and its corresponding temperature are determined by solving the following equation by iteration:

$$h_f(T_{vi} - T_w) = h_{mj} \rho_{vb} \ln \left[\frac{1 - P_{vi}/P}{1 - P_{vb}/P} \right] . \quad (4)$$

The alternative model is the Nusselt model with UCB multipliers, which is revised to include the effects of the interfacial shear and the presence of the noncondensable gas in a vertical tube as follows:

$$h_{UCB} \cdot \frac{\delta}{k_f} = f_1 \cdot f_2 , \quad (5)$$

where f_1 and f_2 are formulated from fits to the experimental data as follows:

$$f_1 = 1 + 2.88 \times 10^{-5} Re_{mix}^{1.18} , \quad (6)$$

and

$$f_2 = \begin{cases} 1 - 10 W_{air} & \text{for } W_{air} < 0.063, \\ 1 - 0.938 W_{air}^{0.13} & \text{for } 0.063 < W_{air} < 0.6, \\ 1 - W_{air}^{0.22} & \text{for } W_{air} > 0.6, \end{cases} \quad (7)$$

where Re_{mix} is the mixture Reynolds number and W_{air} the air mass fraction. The enhancement factor, f_1 , accounts for the effects of the shear of the gas on the liquid film, and the degradation factor, f_2 , accounts for the effects of the noncondensable gas on the heat transfer

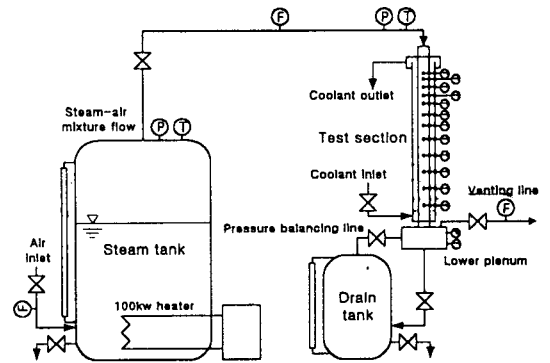


Fig. 1. A schematic Diagram of KAIST Condensation Experimental Apparatus

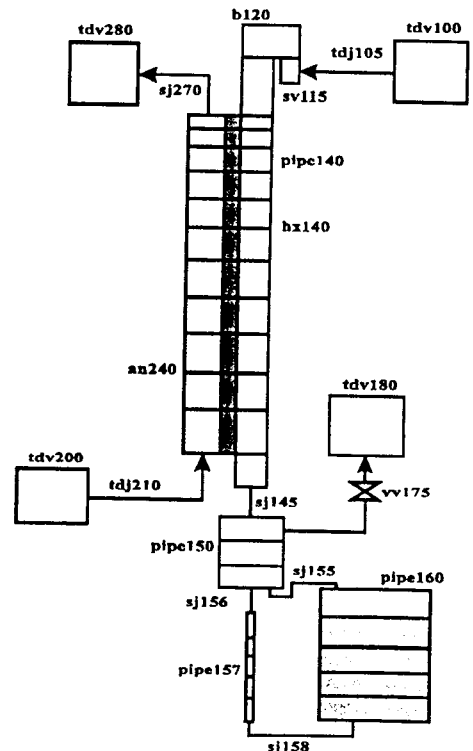


Fig. 2. Nodalization Scheme of RELAP5/MOD3.2 for PCCS Experimental Facility

coefficient. The maximum value allowed for f_1 is 2.0 to prevent over-predicting in the high shear region.

3. Experimental Setup and Modeling

The steam condensation experiments are performed at KAIST[7]. Figure 1 shows the schematic diagram of the experimental facility. The experimental facility consists of a steam tank including a 100kW heater, a steam-noncondensable gas mixture supply line, a test section with a condensing tube and its surrounding coolant jacket, a lower plenum, venting and draining systems, and a unit of data acquisition system.

In the case of *E12b* in KAIST experiments, the experimental procedure is as follows: 1) turn on and control the heater to generate steam to give a predetermined pressure in the steam tank; 2) adjust the coolant flow rate to the determined value; 3) inject the air into the tank to keep a constant initial condition; 4) after readjusting the heater power, vent the accumulated air and drain the condensate to stabilize the system pressure; 5) acquire the steady state data from sensors and transducers; 6) calculate the local heat transfer coefficients and the other reduced data from the raw data.

Figure 2 shows the nodalization scheme of RELAP5/MOD3.2 for the present experimental facility. The present RELAP5/MOD3.2 nodalization used for this simulation contains 41 control volumes, 6 junctions, a valve and a heat structure. Time-dependent volumes acting as infinite sources or sinks are used to represent boundary conditions both for the steam-noncondensable gas mixture flow in a condensing tube and for the coolant flow in a coolant jacket. For the simulation of the coolant jacket, two time dependent volumes 200 and 280 are connected to the annulus 240 with 11 volumes via a time dependent junction 210 and a single junction 270. Similarly, for the simulation of the steam-noncondensable gas mixture flow two time dependent volumes 100 and 180, a pipe with 13

volumes, a time dependent junction 105 and a single junction 151 are also used. A branch 120 is used to simulate an upper plenum and three pipe volumes 150, 160 and 157 are used to simulate a lower plenum, a drain tank and a connecting pipe between the lower plenum and the drain tank, respectively. The above three pipes are connected using single junctions 155, 156 and 158. A valve 175 is used to regulate the venting of the mixture of the residual steam and the noncondensable gas. A heat structure 140 with 11 volumes is used to represent the heat transferred from the steam-noncondensable gas mixture to the coolant through the condensing tube.

4. Results and Discussion

For a base case calculation, an experiment *E12b* in KAIST condensation experiments is simulated by RELAP5/MOD3.2. The experiment *E12b* is performed for the inlet steam-air mixture flow rate of 32.7kg/hr, the inlet air mass fraction of 21.5%, and the inlet saturated steam temperature of 143.4°C. Steady state calculations are performed to determine whether or not it can describe properly the steam condensation experiments in the presence of noncondensables in a vertical tube of PCCS. These simulations use both the default and the alternative models of RELAP5/MOD3.2 to be compared each other and their results are also compared with the experimental data, which are shown in Figures 3 through 7.

The following main characteristics are found:

- 1) Figure 3 shows that the calculated mixture Reynolds number from the default model is always higher than that from the alternative model. The local mixture Reynolds number calculated from the default model decreases more slowly than that from the alternative model throughout the tube. As the amount of

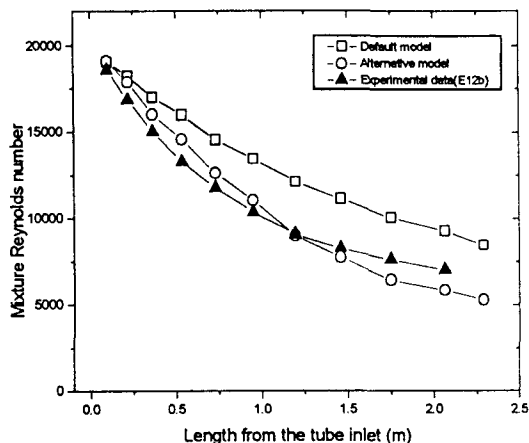


Fig. 3. Comparison of Mixture Reynolds Numbers Calculated Using Two Condensation Models with the Experimental Data of E12b

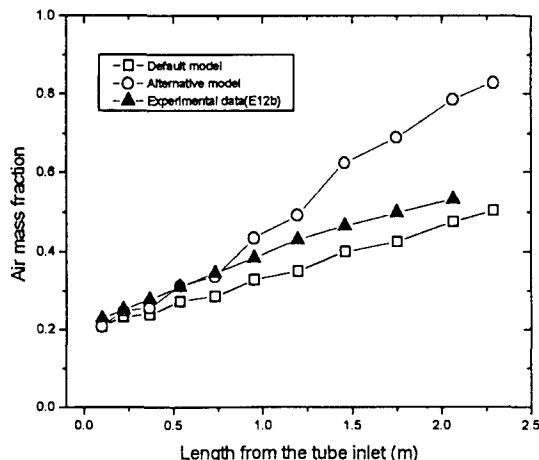


Fig. 4. Comparison of Air Mass Fractions Calculated Using Two Condensation Models with the Experimental Data of E12b

the mass transferred to the liquid film by the steam condensation is large for the simulation using the alternative model, the mixture Reynolds number is calculated to be smaller for the alternative model than for the default model. The experimental data give similar values to the alternative model.

- 2) Figure 4 shows that the calculated air mass fraction from the default model is always lower than that from the alternative model. The experimental air mass fraction is the ratio of air flow rate and total flow rate. The calculated air mass fraction from the default model increases linearly and is always slightly lower than the experimental data. However, the calculated air mass fraction from the alternative model increases rapidly throughout the condensing tube and it always keeps higher values than the experimental data except for the inlet.
- 3) Figure 5 shows the distributions of the saturated steam, the inner tube wall and the coolant bulk temperatures along the condensing tube. All the calculated temperatures from the default model decrease more slowly than those from the

alternative model. So the saturated steam temperature from the default model always keeps a higher value than that from the alternative model, and its coolant bulk temperature always keeps a lower value. The inner wall temperatures from the default model keep lower values than those from the alternative model except for the outlet of the condensing tube. The experimental saturated steam temperature is always similar to that from the default model. The experimental inner wall temperatures keep lower values than those from both the default model and the alternative model, but they crossed with each other in the upper part of the condensing tube. The experimental coolant bulk temperature goes between that from the default model and that from the alternative model along the condensing tube.

- 4) Figure 6 shows that the calculated void fractions from both condensation models are compared with those from the experimental data. The void fraction, α , can be calculated from the known condensate film thickness, δ , and the

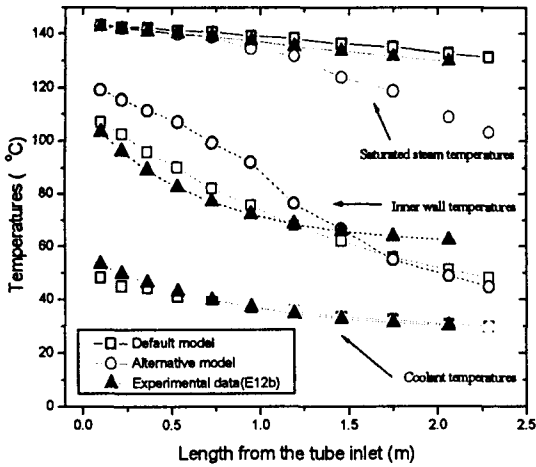


Fig. 5. Comparison of Temperatures Calculated Using Two Condensation Models with the Experimental Data of E12b

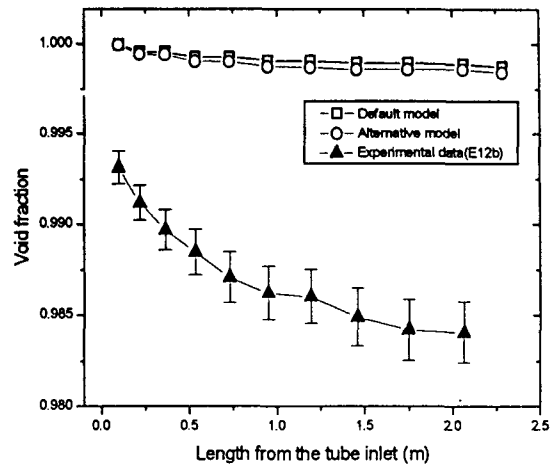


Fig. 6. Comparison of Simulated Void Fractions with KAIST Experimental Data of E12b

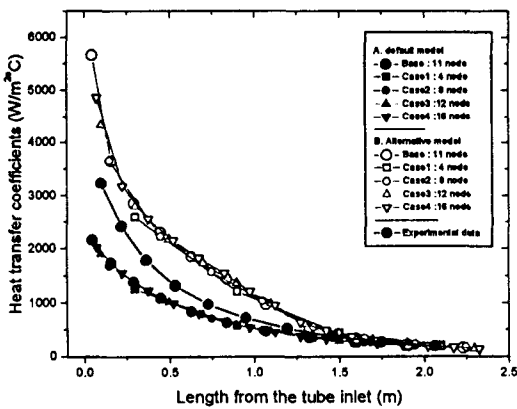


Fig. 7. Comparison of Calculated Heat Transfer Coefficients with the Experimental Data of E12b with the Variation of the Node Number

inner tube diameter, D , as follows:

$$\alpha = 1 - \frac{4 \delta}{D} \quad (8)$$

The condensate film thickness is calculated using Nusselt correlation[8]. The error bars of experimental void fractions are also calculated

from the experimental condensate film thickness and their error bounds. The void fractions calculated from both models of RELAP5/MOD3.2 show much higher values than those from the experimental data. It is due to the fact that two phase wall friction factor in an annular film flow is underestimated by the RELAP5/MOD3.2 code when the condensate film is very thin.

5) Figure 7 shows that the calculated heat transfer coefficient from the default model is always lower than that from the alternative model throughout the condensing tube. The experimental data is always higher than the heat transfer coefficient calculated from the default model, but it is always lower than that calculated from the alternative model. Three heat transfer coefficients, or two simulated results and one experimental data, are greatly different in the inlet of the test section, but they are similar in the outlet of the condensing tube, where the amount of steam is greatly reduced by condensation and the convective heat transfer is dominant. As the default model does not take into account the entrance effect, it

under-predicts the experimental heat transfer coefficient. It is the reason why the default model is a conservative model.

RELAP5/MOD3.2 permits the user to vary the nodalization. By changing the number of nodes in the heat structure, it is possible to investigate whether or not the node number affects the heat transfer characteristics in RELAP5/MOD3.2. There was much effort to eliminate the dependence of RELAP5/MOD3.1 on the node size in condensation heat transfer coefficient for an inclined surface[12]. RELAP5/MOD3.2 calculates the heat transfer coefficient based on the local film thickness instead of the averaged one in RELAP5/MOD3 up to MOD3.1.1.1 version. To investigate the effect of the divided node number, the test section is divided into 4, 8, 12, and 16 nodes regularly instead of the irregular 11 nodes in the base case calculation of *E12b*. Figure 7 shows that the calculated heat transfer coefficients vary little along the condensing tube for the different node numbers. The simulated results show that the change of the node number in the heat structure hardly affects the heat transfer characteristics both in the default and in the alternative model of RELAP5/MOD3.2.

To perform a sensitivity study for input parameters, the following 7 input parameters are varied to compare the calculation results with changes of those parameters: the pressure at the inlet of the test section, P_{in} ; its saturated temperature, T_{in} ; the inlet steam-air mixture flow rate, MF; the inlet air mass fraction, AMF; the temperature at the outlet of the test section, T_{out} ; the temperature at the inlet of the coolant, $T_{c,in}$; the coolant flow rate, CF. The effects of the coolant flow rate, the inlet coolant temperature, and the vented mixture temperature give negligible effects on the heat transfer coefficient in the condensing tube except for the minor variations

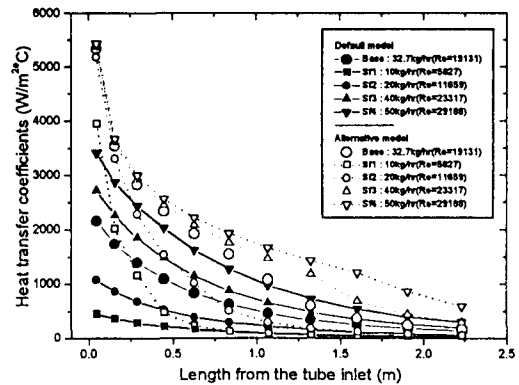


Fig. 8. Comparison of Calculated Heat Transfer Coefficients with the Variation of the Steam-Air Mixture Flow Rate in Default Model

due to the changes of the condition of the coolant. However, the inlet steam-air mixture flow rate, the inlet air mass fraction and the inlet saturated steam temperature give significant changes of the heat transfer coefficient in the condensing tube.

In this study, three main parameters are changed to show their sensitivity. Simulations are performed with two wall film condensation models, the default and the alternative models. The difference between two simulated heat transfer coefficients decreases as the inlet steam-air mixture flow rate increases, the inlet air mass fraction decreases, and the inlet saturated steam temperature decreases. The heat transfer coefficient calculated using the alternative model is always higher than that using the default model, especially in the inlet region of the condensing tube.

The inlet steam-air mixture flow rates vary between 10, 20, 40, and 50kg/hr instead of 32.7kg/hr of the base case of *E12b*, and they are identified as Sf1, Sf2, Sf3, and Sf4, respectively. Figure 8 shows the simulation results of local heat transfer coefficients using both the default and the alternative models. For the simulation using the

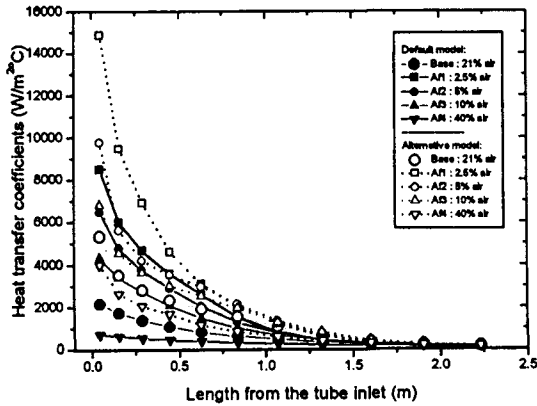


Fig. 9. Comparison of Calculated Heat Transfer Coefficients with the Variation of the Inlet Air Mass Fraction in Default Model

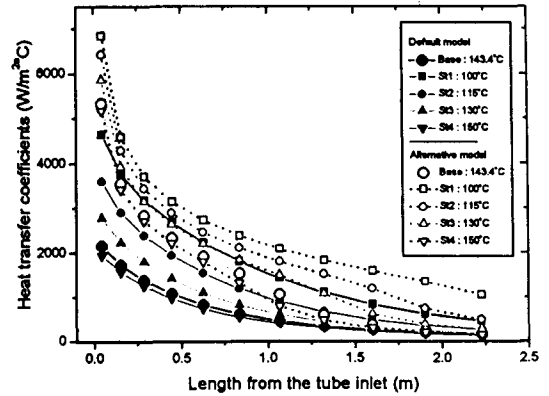


Fig. 10. Comparison of Calculated Heat Transfer Coefficients with the Variation of the Inlet Saturated Temperature in Default Model

default model, the local heat transfer coefficient increases throughout the condensing tube with the increase of the inlet steam-air mixture flow rate, and it increases much especially in the inlet region. However, for the simulation using the alternative model, it is independent of the inlet steam-air mixture flow rate in the inlet of the tube, but it is very much changed in the middle of the condensing tube. The two simulated heat transfer coefficients are greatly different in the inlet region, but they are similar in the outlet region of the condensing tube. As the inlet mixture flow rate increases, the heat transfer coefficient using the default model increases to be similar with that using the alternative model. Particularly with the low steam-air mixture flow rate, the simulated heat transfer coefficients by the alternative model are much higher than those by the default model. The alternative model allows the maximum value of 2.0 for f_1 to prevent over-predicting in the high shear region. The corresponding mixture Reynolds number is 7046.5, which can be calculated by Equation 6. When the mixture Reynolds number exceeds the limit of 7046.5, every heat transfer coefficient is doubled regardless of the different

mixture Reynolds numbers. It is the main cause of the over-prediction of heat transfer coefficient by the alternative model. The degradation factor f_2 accounts for noncondensable gas effects on condensation heat transfer coefficient. The heat transfer coefficient is greatly decreased with small amounts of noncondensable gas. The effect is properly correlated by the f_2 factor in the alternative model.

The inlet air mass fractions vary between 2.5, 5, 10, and 40% instead of 21.5% of the base case of *E12b*, and they are identified as Af1, Af2, Af3, and Af4, respectively. Figure 9 shows the simulation results of local heat transfer coefficients using both the default and the alternative models. For the simulations using both the default model and the alternative model, the heat transfer coefficients decrease greatly in the inlet region of the condensing tube with the increase of the air mass fraction, but they are similar in the outlet region. However, the heat transfer coefficient calculated using the default model is always lower than that using the alternative model except for the lower part of the condensing tube. The different inlet air mass fractions affect the heat transfer coefficient

Table 1. The CPU Time and the Grind Time of Various Simulations

I.D.	Node	Problem time(s)	The alternative model			The default model		
			CPU time(s)	No. of time step	Grind time	CPU time(s)	No. of time step	Grind time
E12b	42	250	1511.6	11647	3.090	1790.1	11668	3.653
Nd1	35	250	1053.1	11772	2.556	1127	11337	2.840
Nd2	39	250	1380.8	12276	2.884	1576.7	12002	3.368
Nd3	43	250	1680.6	12389	3.155	1928.8	11779	3.808
Nd4	47	250	1862.7	11649	3.402	2289.8	11659	4.179
Sf1	42	250	849.4	6854	2.951	728.7	4940	3.512
Sf2	42	250	990.9	7995	2.951	1174.8	7903	3.539
Sf3	42	250	1870.3	14974	2.974	2275.6	14843	3.650
Sf4	42	250	2501.7	19888	2.995	3019.9	19850	3.622
Af1	42	250	4463.4	36664	2.899	5415.8	36578	3.525
Af2	42	250	3552.8	29639	2.854	4243.1	29052	3.477
Af3	42	250	1997.7	16033	2.967	2307.2	15958	3.442
Af4	42	250	1193.6	9369	3.033	1376.3	9094	3.603
St1	42	250	2587.1	19866	3.101	2364.7	15628	3.603
St2	42	250	1858.3	15328	2.887	2344.7	15276	3.655
St3	42	250	1863.4	15157	2.927	2302.4	15112	3.628
St4	42	250	1202	9728	2.942	1404.5	9593	3.486

greatly in the upper part of the condensing tube, but they do negligibly in the lower part.

The inlet saturated steam temperatures vary between 100, 115, 130, and 150 °C instead of 143.4 °C of the base case of E12b, and they are identified as St1, St2, St3, and St4, respectively. Figure 10 shows the simulation results of local heat transfer coefficients using both the default and the alternative models. For the simulation using the default model, the heat transfer coefficient decreases greatly with the increase of the inlet saturated steam temperature in the inlet region of the condensing tube, but it changes little in the outlet region. However, for the simulation using the alternative model, the heat transfer coefficient decreases a little with the increase of the inlet saturated steam temperature in the upper part of the condensing tube, but it decreases much

in the lower part.

To perform the above simulations, SUN SPARC 10 is used: its operating system is SunOS 4.1.3-KL; its random access memory is 32 Mbyte; its calculation speed is 86.1MIPS; its clock speed of CPU is 36MHz. The CPU time, the time step size, and the grind time are compared between both calculation results calculated with different wall film condensation models. The required CPU times increase linearly for both the default and the alternative models, except for the initial transient situation. The CPU time shows to change greatly near 10sec when the steady state is achieved. In the steady state the main hydraulic parameters such as system pressure, temperatures and air mass fraction are little changed. When the default model is used, the required CPU time is slightly longer than that of the alternative model. The time

steps fluctuate between 0.00625, 0.0125, and 0.025sec for both the default and the alternative models. When the default condensation model is used, the time step size is smaller, and its fluctuation is more frequent than that of the alternative model. The time step determined by the default model shows to scatter much more than that with the alternative model. It validates the larger fluctuation of the time step and the longer required CPU time.

The grind time is expressed as follow[13]:

$$\text{Grind time} = \frac{\text{CPU} \times 10^3}{C \times \Delta T}, \quad (9)$$

where CPU is the CPU time, C the total number of nodalized volumes, and ΔT the number of time steps. It means the CPU time used for calculating a volume during a second. Table 1. shows the required CPU time and the grind time for the simulations for the sensitivity study. The required CPU time is highest when the inlet mixture flow rate is highest and both the inlet air mass fraction and the inlet saturated steam temperature are lowest. The grind time of the default model is about 23% higher than that of the alternative model.

5. Conclusions

Two wall film condensation models of RELAP5/MOD3.2 are assessed and compared each other with the experiment for condensation heat transfer in the presence of noncondensable gas. After the experimental apparatus being modeled with RELAP5/MOD3.2, the simulation results are compared between two wall film condensation models, and they are also compared with the experimental data.

From the studies, the followings are concluded:

- 1) The default model of RELAP5/MOD3.2 under-predicts the heat transfer coefficients, but its alternative model over-predicts them throughout the condensing tube. Both wall film condensation models over-predict the void fraction due to the underestimated two-phase friction factor.
- 2) The change of the divided node number in heat structure has little influence on the simulation results of the condensation phenomena with RELAP5/MOD3.2 for both of the default and alternative models.
- 3) Through sensitivity study both models show the similar tendencies that the heat transfer coefficients increase as the inlet steam-air mixture flow rate increases, the inlet air mass fraction decreases, and the inlet saturated steam temperature decreases. The difference between the default and alternative models is lowest in the range of high heat transfer coefficients but highest in the range of low heat transfer coefficients.
- 4) Run statistics show that the grind time of the default model is always higher than that of the alternative model by about 23%, and the required CPU time is highest when the inlet steam-air mixture flow rate is highest and both the inlet air mass fraction and the inlet saturated steam temperature are lowest.

References

1. S.H. Chang, H.C. NO, W.P. Baek, S.I. Lee, and S. W. Lee, "Korea Looks Beyond the Next Generation," *Nuclear Engineering International* **12** (1997).
2. S.W. Lee, W.P. Baek, and S.H. Chang, "Assessment of Passive Containment Cooling Concepts for Advanced Pressurized Water Reactors," *Annals of Nuclear Energy* **24** No.6, p.467 (1997).
3. K.Y. Choi, H.S. Park, S.J. Kim, H.C. NO, and

- Y.S. Bang, "Assessment and Improvement of Condensation Models in RELAP5/MOD3.2," *Nuclear Technology* **124 No.2**, p.103 (1998).
4. V.H. Ransom, J.A. Trapp, and R.J. Wagner, "RELAP5/MOD3.2 Code Manual, Volume IV: Models and Correlations," *NUREG/CR-5535, INEL-95/0174*, INEL. (1995).
 5. M. Siddique, M.W. Golay, and M.S. Kazimi, "Local Heat Transfer Coefficients for Forced-Convection Condensation of Steam in a Vertical Tube in the Presence of a Noncondensable Gas," *Nuclear Technology* **102**, p.386 (1993).
 6. S.Z. Kuhn, "Investigation of Heat Transfer from Condensing Steam-Gas Mixtures and Trubulent Films Flowing Downward Inside a Vertical Tube," *PhD Thesis*, Nuclear Engineering, University of California-Berkeley (1995).
 7. H.S. Park, H.C. NO, Y.S. Bang, K.W. Seul, and H.J. Kim, "Assessment of RELAP5/MOD3.2 for Steam Condensation Experiments in the Presence of Noncondensables in a Vertical Tube of PCCS," *NUREG/IA-0147*, U.S. NRC. (1998).
 8. W.A. Nusselt, "The Surface Condensation of Water Vapor," *Z. Ver. Deutsch. Ing.* **60**, p.541 (1916).
 9. M.M. Shah, "A General Correlation for Heat Transfer During Film Condensation Inside Tubes," *Int. J. Heat Mass Transfer* **22**, p.547 (1979).
 10. A.P. Colburn and O.A. Hougen, "Design of Cooler Condensers for Mixtures of Vapors with Non-Condensing Gases," *Industrial and Engineering Chemistry* **26** No.11, p.1178 (1934).
 11. W.M. Rohsenow and Y.H. Choi, *Heat Mass and Momentum Transfer*, New Jersey, Prentice-Hall (1961).
 12. H.T. Kim and H.C. NO, "Modification of Condensation Heat Transfer Model of RELAP5/MOD3.1 for the Simulation of Secondary Condensers," *Nuclear Technology* **119**, p.98 (1997).
 13. S.I. Lee and H.C. NO, "Assessment of RELAP5/MOD3.1 for Direct-Contact Condensation in the Core Makeup Tank of the CARR Passive Reactor," *Annals of Nuclear Energy* **24 No.7**, p.553 (1997).